APPLIED AND ENVIRONMENTAL MICROBIOLOGY, Nov. 2010, p. 7217–7225 Vol. 76, No. 21
0099-2240/10/$12.00 doi:10.1128/AEM.00985-10

The *Rhodococcus opacus* PD630 Heparin-Binding Hemagglutinin Homolog TadA Mediates Lipid Body Formation▽

Daniel P. MacEachran,[1] M. E. Prophete,[1] and A. J. Sinskey[1,2,3]*

Department of Biology,[1] Division of Health Sciences and Technology,[2] and Engineering Systems Division,[3] Massachusetts Institute of Technology, Cambridge, Massachusetts

Received 22 April 2010/Accepted 1 September 2010

Generally, prokaryotes store carbon as polyhydroxyalkanoate, starch, or glycogen. The Gram-positive actinomycete *Rhodococcus opacus* strain PD630 is noteworthy in that it stores carbon in the form of triacylglycerol (TAG). Several studies have demonstrated that *R. opacus* PD630 can accumulate up to 76% of its cell dry weight as TAG when grown under nitrogen-limiting conditions. While this process is well studied, the underlying molecular and biochemical mechanisms leading to TAG biosynthesis and subsequent storage are poorly understood. We designed a high-throughput genetic screening to identify genes and their products required for TAG biosynthesis and storage in *R. opacus* PD630. We identified a gene predicted to encode a putative heparin-binding hemagglutinin homolog, which we have termed *tadA* (*t*riacylglycerol *a*ccumulation *d*eficient), as being important for TAG accumulation. Kinetic studies of TAG accumulation in both the wild-type (WT) and mutant strains demonstrated that the *tadA* mutant accumulates 30 to 40% less TAG than the parental strain (WT). We observed that lipid bodies formed by the mutant strain were of a different size and shape than those of the WT. Characterization of TadA demonstrated that the protein is capable of binding heparin and of agglutinating purified lipid bodies. Finally, we observed that the TadA protein localizes to lipid bodies in *R. opacus* PD630 both *in vivo* and *in vitro*. Based on these data, we hypothesize that the TadA protein acts to aggregate small lipid bodies, found in cells during early stages of lipid storage, into larger lipid bodies and thus plays a key role in lipid body maturation in *R. opacus* PD630.

While the majority of eubacteria (24, 33), and indeed many archaea (22, 33), store carbon as polyhydroxyalkanoate (PHA), a small subset of organisms, primarily actinomycetes, are capable of storing carbon in the form of triacylglycerol (TAG). TAG biosynthesis and storage has been observed in members of the genera *Mycobacterium*, *Rhodococcus*, *Streptomyces*, *Nocardia*, and others (4, 6, 11, 12, 19, 20, 36). Of these organisms, TAG biosynthesis and storage has been most extensively studied for the Gram-positive, non-spore-forming actinomycete *Rhodococcus opacus*, strain PD630 (1–6, 11, 12, 19, 20, 25, 36, 38–41).

Several studies have demonstrated that *R. opacus* PD630 is capable of accumulating up to 76% of its cell dry weight (CDW) as TAG (summarized in reference 3). As is the case for PHA biosynthesis, TAG accumulation occurs during nitrogen starvation when carbon is in excess (1–3, 27, 41). Paralleling PHA biosynthesis further, TAG is stored in *R. opacus* PD630 in distinct inclusion bodies, termed lipid bodies (2, 3, 25, 38, 40). While several studies have sought to identify the underlying molecular and biochemical mechanisms behind TAG biosynthesis and storage in the form of lipid bodies, very little is known concerning these processes.

We sought to identify genes and their products that are essential for lipid metabolism in *R. opacus* PD630. Utilizing a forward genetic approach, we identified a conserved hypothetical gene, termed herein *tadA* (*t*riacylglycerol *a*ccumulation *d*eficient), which is predicted to encode a protein with sequence similarity to the heparin-binding hemagglutinin (HbhA) family of proteins from the genus *Mycobacterium*. The *tadA*::Tn*5* mutant accumulates 30 to 40% less TAG than the parental strain. We demonstrate that this deficiency is most likely the result of altered lipid body formation and morphology. Through biochemical studies, we further demonstrate that the predicted heparin-binding activity of this protein is essential for its activity both *in vivo* and *in vitro*. To our knowledge, this is the first protein shown to regulate lipid body assembly and maturation in prokaryotes.

MATERIALS AND METHODS

Bacterial strains, chemicals, and media. All bacterial strains, plasmids, and oligonucleotides used in this study are listed in Table 1. Bacteria were propagated in lysogeny broth (LB) (7) (Difco, Lawrence, KS) or minimal medium, unless otherwise noted. The minimal medium was prepared as previously described (27) and supplemented with 4% glucose and 0.15% ammonium sulfate. Growth medium was supplemented with kanamycin (100 μg/ml), gentamicin (10 μg/ml), ampicillin (150 μg/ml), and/or arabinose (0.2%). All restriction enzymes were purchased from New England BioLabs (Ipswich, MA). Chemicals were purchased from Sigma-Aldrich (St. Louis, MO). Plasmids were constructed with either *Saccharomyces cerevisiae* using *in vivo* recombinational cloning (34, 35) or *Escherichia coli* EC100D (Epicentre Biotechnologies, Madison, WI) using standard techniques. Plasmid DNA was mobilized into *R. opacus* PD630 using electroporation as described below. Plasmid DNA was purified from cells using Qiagen mini-prep kits (Qiagen, Valencia, CA) per the manufacturer's instructions.

Electroporation of DNA into *R. opacus* PD630. Electrocompetent *R. opacus* cells were obtained by centrifuging 3 ml of 48-h-old cultures grown in LB medium supplemented with 1% Casamino Acids followed by several washes in sterile distilled H_2O (dH_2O), and cell pellets were then resuspended in 200 μl of sterile dH_2O to which 1 μg of plasmid DNA was added. Electroporations were performed using a Bio-Rad gene pulser (Hercules, CA) apparatus set to 2.5 kV, 25 μF, and 600 Ω. Following electroporation, cells were immediately resuspended in 2 ml of LB medium and incubated at 30°C for 2 h prior to plating on selective medium.

* Corresponding author. Mailing address: Department of Biology, Massachusetts Institute of Technology, Cambridge, MA 02139. Phone: (617) 253-6721. Fax: (617) 253-8550. E-mail: asinskey@mit.edu.

▽ Published ahead of print on 17 September 2010.

TABLE 1. Strains, plasmids, and primers used

Strain, plasmid, or primer	Relevant genotype or primer sequence	Source or reference
Strains		
E. coli		
TOP10	*ara* mutant	Invitrogen
DPM229	*E. coli* Top10, pDPM72	This study
DPM238	*E. coli* Top10, pDPM75	This study
Rhodococcus		
R. opacus PD630	Wild-type	3
DPM245	Wild-type *R. opacus*, pDPM70	This study
DPM246	Wild-type *R. opacus*, p*tadA*	This study
DPM247	Wild-type *R. opacus*, p*tadA*ΔC	This study
DPM248	*tadA*::Tn*5*, pDPM70	This study
DPM249	*tadA*::Tn*5*, p*tadA*	This study
DPM250	*tadA*::Tn*5*, p*tadA*ΔC	This study
Plasmids		
pAL358	*Rhodococcus*/*E. coli* shuttle vector, Gm^r	43
pMSG374	*Mycobacterium* expression vector	37
pMQ70	*S. cerevisiae*/*E. coli* expression vector, Ap^r	34
pDPM70	*S. cerevisiae*/*Rhodococcus*/*E. coli* expression vector, Gm^r	This study
p*tadA*/pDPM78	pDPM70 + *R. opacus* PD630 *tadA*, Gm^r	This study
p*tadA*ΔC/pDPM80	pDPM70 + ΔC-terminus *tadA*, Gm^r	This study
pDPM72	pMQ70 + *tadA* C-terminal six-histidine fusion, Ap^r	This study
pDPM76	pMQ70 + TadA ΔC-terminus C-terminal six-histidine fusion, Ap^r	This study
Primers		
pDPM65 for	5′-CGGATCTGCCCTGGCTTCAGGAGATCGGAAGACGTGAGCGGATAACAATTTCACACAGG-3′	
pDPM65 rev	5′-CGAATTGCTGCGCGTAACCACCACACCCGCCGCGCTTAGGATCGTCGGCACCGTCACGG-3′	
pDPM66 for	5′-GCTCGAGGCATGCAGAAAGGAGGCCATATGGGACTGCATGCATCATCATCATCATCATCATATGACTGACCAGAAGACCATCGAC-3′	
pDPM66 rev	5′-CCATGATTACGCCAAGCTTGGTACCGAGCTCGGTTCAAGCCTTCTTGGCCGGAGCAGCC-3′	
pDPM80 rev	5′-ATGACCATGATTACGCCAAGCTTGGTACCGAGCTCGGTTCAGTCGGCCTGAGCCTGGACGTCGG-3′	
pDPM65 seq for	5′-GGCAAAATGGTGGAAGGGCG-3′	
pDPM65 seq rev	5′-GGCCTTGCTGTTCTTCTACGGC-3′	
pDPM72 for	5′-CAAAACAGCCAAGCTTTTAATGATGATGATGATGATGAGCCTTCTTGGCCGGAGCAGCC-3′	
pDPM72 rev	5′-TACCCGTTTTTTTGGGCAGCGAATTCAGGAGGTCTCTCTCATGACTGACCAGAAGACCATCGACAGC-3′	
pDPM75 rev	5′-CGCCAAAACAGCCAAGCTTTTAATGATGATGATGATGGTCGGCCTGAGCCTGGACGTCGGCAGCGGTGGCGGCGACGC-3′	
pMQ70 seq for	5′-CAGACCGCTTCTGCGTTCTGATTTAATCTG-3′	
pMQ70 seq rev	5′-CGCTAACCAAACCGGTAACCCCGC-3′	

Transposon mutagenesis and screening. The EZ-Tn*5* Transposome system from Epicentre Biotechnologies (Madison, WI) was used to introduce random mutations throughout the *R. opacus* PD630 genome. Following electroporation as described above, with the Transposome system, transformants were plated on solidified LB medium supplemented with kanamycin and incubated at 30°C for 3 to 4 days. Colonies were transferred to 96-well plates containing LB medium supplemented with kanamycin and incubated at 30°C for 4 days. Following growth, mutants were screened as described below.

Mapping transposon insertion sites. Identification of the transposon insertion site was performed using a modified marker rescue technique as described by the manufacturer. Genomic DNA was purified as previously described (23). Following purification, genomic DNA was digested with the restriction endonuclease AgeI. Digested genomic DNA was then ligated using T4 DNA ligase and electroporated into *E. coli* EC100D cells and grown on solid LB medium supplemented with kanamycin. Following growth, single colonies were then grown in liquid LB medium supplemented with kanamycin, from which plasmid DNA was purified and sequenced using primers provided by the Transposome manufacturer.

TAG accumulation screening. Mutants were transferred from 96-well dishes to solid minimal medium supplemented with 4% glucose and 0.15% ammonium sulfate and grown for 120 h at 30°C. Following growth, plates were flooded with 0.2% Sudan Black in 95% ethanol and incubated at room temperature for 15 min followed by three 95% ethanol washes for 1, 5, and 15 min each. Mutants were selected based on their reduced staining with the dye.

Lipid extraction and thin-layer chromatography. Extraction of lipids from cultures was performed as previously described with minor modifications (8). Thin-layer chromatography (TLC) experiments were performed using a two-step resolution method as previously described (14, 26). Equal volumes of lipid extract were spotted onto glass-backed silica gel 60 TLC plates (EMD Chemicals Inc., Gibbstown, NJ) and dried under a constant stream of nitrogen. Samples were resolved using an initial polar solvent system consisting of 60:35:5 chloroform/methanol/water, dried, and then further resolved using a second solvent

system containing 70:30:1 hexane/diethyl ether/acetic acid. Plates were developed by charring by first exposing the plates to a 3% cupric acetate–8% aqueous phosphoric acid solution followed by baking in a 200°C oven. Glycerol monooleate, glycerol dioleate, and glycerol trioleate were used as standards.

GC-FAMES. Cell pellets for gas chromatography of fatty acid methyl esters (GC-FAMES) analysis were lyophilized overnight. Extraction and subsequent transesterification of fatty acids was performed as previously described (9, 27). Samples were analyzed using a Hewlett-Packard 6890 gas chromatograph with an Agilent DB-Wax megabore column (30 m by 0.53 mm by 1 μm). Methyl esters were detected using a flame ionization detector. The oven temperature was ramped from 70 to 220°C for all samples. Total fatty acids as well as the abundance of various species were determined by comparing the resulting chromatograph peak areas to a series of standards.

Construction of plasmids pDPM70, pDPM78, and pDPM80. The *Rhodococcus*/*E. coli*/*S. cerevisiae* expression vector pDPM70 was constructed using *in vivo* recombination as previously described (34, 35). The *URA3* gene and the *CEN6*/*ARSH4 S. cerevisiae* origin of replication from pMQ30 (34) was amplified using the primers pDPM13 for and pDPM13 rev and subsequently cloned into the *Rhodococcus*/*E. coli* shuttle vector pAL358, creating the *Rhodococcus*/*E. coli*/*S. cerevisiae* shuttle vector pDPM13. The P*smyctetRO* promoter and cognate ribosome binding site were amplified from pMSG374 (15, 37) using primers pDPM65 for and pDPM65 rev and were cloned into pDPM13, which had previously been linearized via restriction digestion.

Full-length *tadA* was amplified from the *R. opacus* PD630 chromosome and integrated downstream of the P*smyc* promoter in pDPM70 using primers pDPM66 for and pDPM66 rev to create the *Rhodococcus tadA* expression plasmid pDPM78. To create the ΔC-terminal TadA mutant protein (or mutein), the *tadA* gene was amplified from the *R. opacus* PD630 chromosome using primers pDPM66 for and pDPM80 rev and cloned into pDPM70, thus creating plasmid pDPM80.

Plasmid pDPM72, containing the full-length wild-type (WT) *tadA* open reading frame with a C-terminal hexahistidine tag, was created using *in vivo* recombination cloning. The *tadA* gene was amplified from the *R. opacus* PD630 chromosome using primers pDPM72 for and pDPM72 rev and subsequently cloned into pDPM77 (29), which had been previously linearized via restriction digestion. To create pDPM75, containing a hexahistidine-tagged C-terminal truncation of TadA, pDPM72 was linearized utilizing the restriction enzyme SphI, which cleaves pDPM72 within the 3′ end of the *tadA* open reading frame, and subsequently recombined with the primer pDPM75 rev in *S. cerevisiae*.

Fluorescence microscopy. Nile Red staining of cells was performed as previously described (18, 21). Briefly, cultures were mixed 1:1 with a 75% glycerol solution containing 5 μg of the lipophilic fluorophore Nile Red and observed using a Carl Zeiss AX10 Imager.A1 fluorescence microscope using green fluorescent protein (GFP) and cy3 filters. Images were recorded using a Carl Zeiss AxioCam MRm (Carl Zeiss Microimaging, Inc., Thornwood, NY) and subsequently analyzed using Adobe Photoshop CS3.

Purification of lipid bodies. Lipid bodies were purified from *R. opacus* PD630 as previously described (25) with minor modifications. *R. opacus* was grown for 96 h in minimal medium supplemented with 4% glucose and 0.15% ammonium sulfate. Cultures were harvested via centrifugation at 6,000 × *g* for 20 min. Cell pellets were resuspended in 25 ml of phosphate-buffered saline (PBS) and lysed by passing through a French pressure cell set at 18,000 lb/in^2 five times. An equal volume of 80% glycerol was added to lysates followed by centrifugation at 6,000 × *g* for 3 h at 4°C. Following centrifugation, the upper layer (lipid body fraction) was removed and resuspended in 40 ml of 40% glycerol (tube 1), and the pellet (cell debris) was resuspended in 40 ml of 40% glycerol (tube 2), followed by a second centrifugation of both tubes at 6,000 × *g* for 3 h. The lipid body layer (upper layer) from tube 1 was removed and placed in 20 ml PBS, and the cell debris (pellet) from tube 2 was resuspended in 20 ml of PBS, followed by centrifugation of both tubes at 7,500 × *g* for 30 min. All fractions were then resuspended in 5 ml of PBS and used immediately.

Purification of TadA. TadA was purified by nickel affinity chromatography as previously described (29, 31) using a 5-ml HisTrap fast-flow nickel affinity column (GE Healthcare, Piscataway, NJ). TadA-containing fractions were pooled and concentrated using Vivaspin15R columns with a molecular weight cutoff of 10,000 (Sartorius Stedim, Goettingen, Germany) and dialyzed against 20 mM Tris (pH 7.0)–100 mM NaCl using Slide-A-Lyzer dialysis cassettes (Thermo Scientific, Rockford, IL). Protein concentrations were determined using a Bio-Rad protein assay kit (Bio-Rad, Hercules, CA) per the manufacturer's instructions, with bovine serum albumin serving as a protein standard.

Heparin-Sepharose binding. Purified TadA was diluted to a final concentration of 500 μg/ml in dialysis buffer. A 100-mg portion of heparin-Sepharose CL-6B (GE Healthcare, Piscataway, NJ) was resuspended in 5 ml of Tris buffer (20 mM Tris [pH 7.0], 100 mM NaCl) and allowed to rehydrate with gentle agitation for 1 h. After rehydration, the resin was pelleted via centrifugation at 1,000 × *g* for 2 min and subsequently washed 3 times in the same buffer. The resin was resuspended in 1 ml of Tris buffer to which 500 μg of purified TadA was added. The Sepharose-TadA slurry was incubated at 4°C for 1 h with gentle agitation. Following incubation, the resin was pelleted, an aliquot of the supernatant was removed (flowthrough fraction), the Sepharose was washed 5 times with Tris buffer, and an aliquot of the supernatant from the final wash was removed (wash fraction). The remaining heparin-Sepharose was resuspended in 1 ml of Tris buffer from which an aliquot was removed (bead fraction). SDS-PAGE loading buffer was added to each aliquot, and the aliquots were then boiled for 5 min. Samples were resolved using 10% acrylamide Ready gel Tris-HCl SDS-PAGE gels (Bio-Rad, Hercules, CA) and stained using colloidal Coomassie as previously described (17, 28).

Lipid aggregation assays. Purified lipid bodies were diluted to a final optical density at 600 nm of 1.0, mixed with either 20 mM Tris, 100 mM NaCl, or purified TadA in a round-bottom 96-well dish, and incubated at room temperature for 12 h. Wells were imaged using a Canon Powershot SD1200 IS digital camera (Canon, Lake Success, NY). To obtain a more quantitative measure of aggregation, 2 μl of the supernatant was removed from each well, and the optical density at 600 nm was determined using a Nano-Drop spectrophotometer (Thermo Scientific, Wilmington, DE).

Western blotting. All Western blotting was performed as previously described (10, 29). Qiagen Penta-His antibodies (Qiagen, Valencia, CA) were used at a dilution of 1:3,000 as the primary antibody in all Western blots. Goat anti-rabbit horseradish peroxidase (HRP)-conjugated antibodies (Bio-Rad, Hercules, CA) were used as the secondary antibody for all Western blots.

Nucleotide sequence accession number. The *tadA* sequence was submitted to GenBank under accession number HM625859.

RESULTS

Genetic screening for *tad* mutants. A library of 5,000 random Ez-Tn*5* *R. opacus* PD630 mutants was generated and subsequently screened for triacylglycerol biosynthesis using a Sudan Black-based screening method. Previous experiments by Kurosawa and colleagues as well as Alvarez et al. (2, 3, 27) demonstrated that *R. opacus* accumulates high concentrations of TAG when grown in medium with a high carbon/nitrogen ratio. Accordingly, our Tn*5* mutants were grown on minimal medium supplemented with 4% glucose and 0.15% ammonium sulfate for 120 h, allowing for significant TAG accumulation. Following growth, accumulated TAG was detected by staining the colonies with the lipophilic dye Sudan Black B. TAG accumulation was exhibited by dark blue staining of the colonies, as seen in the wild-type example in Fig. 1A; mutants deficient in TAG accumulation exhibited less staining, as is shown for the 19A3 mutant in Fig. 1A. From this initial screening, we identified several mutants that demonstrated various degrees of decreased staining compared to the wild type.

As decreased staining could readily be due to a variety of different factors other than a loss of TAG accumulation, mutants of interest were subjected to a second round of screening wherein they were grown in minimal medium in flasks for 120 h and then analyzed for their TAG content using TLC. Of the initial strains assayed, one, designated 19A3, demonstrated wild-type-like growth while accumulating 35% less TAG than did the wild-type strain.

Kinetics of TAG accumulation in the wild-type and 19A3 mutant strains. Following the secondary screening, we sought to better characterize the 19A3 mutant by studying the kinetics of TAG accumulation. Wild-type *R. opacus* PD630 and the 19A3 mutant strain were grown in minimal medium supplemented with 4% glucose and 0.15% ammonium sulfate. Samples were removed at 24, 48, 72, 96, and 120 h to measure the

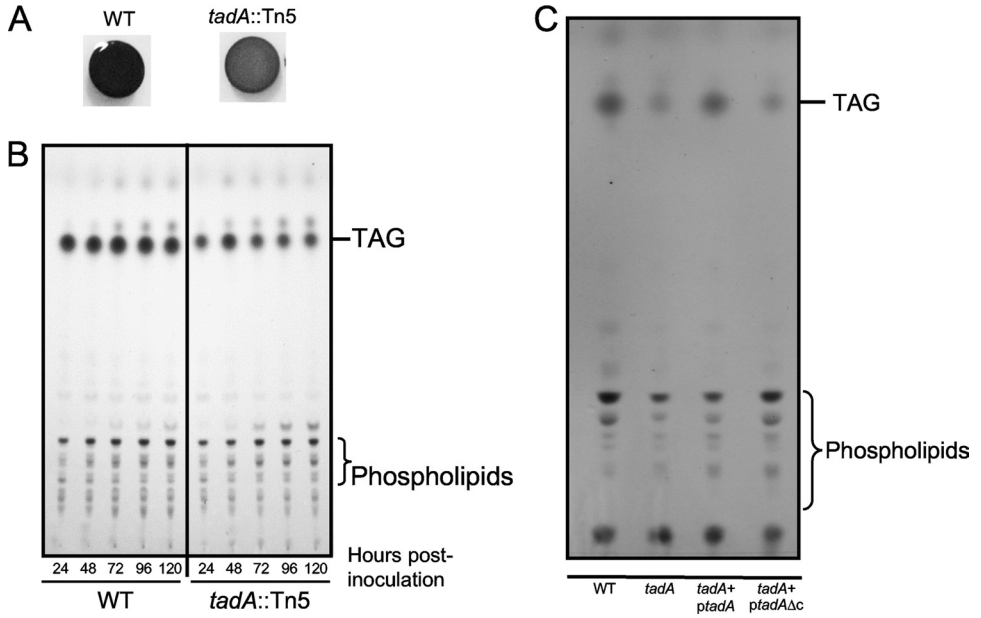

FIG. 1. The *tadA*::Tn*5* mutant is deficient for TAG accumulation. (A) Sudan Black B-stained colony phenotype of wild-type *R. opacus* and the *tadA*::Tn*5* mutant. Colonies were grown for 120 h and stained with the lipophilic dye Sudan Black B. The lighter staining of the *tadA*::Tn*5* mutant is suggestive of decreased TAG accumulation. (B) Thin-layer chromatography analysis of lipids in wild-type *R. opacus* and the *tadA*::Tn*5* mutant. Strains were grown in minimal medium, and samples were removed and lyophilized at 24, 48, 72, 96, and 120 h, followed by resolution using TLC. The *tadA*::Tn*5* mutant demonstrates decreased TAG accumulation at all time points compared to the parental strain. (C) Complementation analysis of the *tadA*::Tn*5* mutant. Expression of wild-type *tadA* (p*tadA*), but not the truncation mutant (p*tadA*ΔC), compensated for the observed decrease in TAG accumulation in the *tadA*::Tn*5* mutant.

culture turbidity (A_{600}), determine the CFU, measure nitrogen and glucose concentrations as well as pH, and assess TAG accumulation. Whereas the numbers of CFU, as well as the consumption of nitrogen and glucose, were identical between the two strains (data not shown), there was a distinct difference in the culture turbidity and the amount of TAG accumulated. We observed that at later time points, the wild-type strain had a higher optical density (72 h, 8.75 ± 0.34; 96 h, 8.80 ± 0.47; and 120 h, 9.08 ± 0.26) than the mutant strain (72 h, 8.22 ± 0.43; 96 h, 8.31 ± 0.19; and 120 h, 8.09 ± 0.31). TLC analysis of the lipid content of the two strains demonstrated that the concentrations of the polar lipids, thought to consist primarily of phospholipids and acting as a convenient loading control, remained similar between the two strains. However, the mutant strain demonstrated a reduction in TAG compared to its wild-type counterpart (Fig. 1B). A densitometric analysis of the TLC results suggests a 30 to 40% reduction in TAG accumulation in the mutant strain. We believe that the optical density difference between the two strains was most likely the result of the decreased accumulation of TAG in the mutant strain and not a difference in growth, a point which was confirmed by CFU counts (data not shown). Interestingly, similar discrepancies in optical density have been described for bacteria accumulating PHAs (42).

We utilized gas chromatography as a second method to analyze the fatty acid content of both the wild type and the mutant strain. Cell pellets from the kinetic experiments, identical to those described above, were lyophilized, and the fatty acids were extracted and converted to fatty acid methyl esters (FAMES) for use in GC. Consistent with our TLC results, we found that the mutant accumulated 38% less fatty acid than the wild type at the 96-h time point (41.2% ± 3.296% FAMES [CDW] for the wild type and 25.54% ± 2.61% FAMES [CDW] for the 19A3 strain). Thus, GC-FAMES analysis confirmed that the 19A3 mutant accumulates 35 to 40% less TAG than the wild-type strain.

Utilizing a marker rescue-like approach, we identified the transposon insertion site in the 19A3 mutant as being 150 nucleotides downstream of the predicted start codon of a gene termed herein *tadA* (*t*riacyglycerol *a*ccumulation *d*eficient), which is predicted to encode a hypothetical protein with sequence similarity to the heparin-binding hemagglutinin family of proteins from mycobacteria (Fig. 2). A BLAST analysis of the nucleotide sequence of the *tadA* gene against the *Rhodococcus jostii* RHA1 genome (http://www.rhodococcus.ca) identified a homolog with 97.46% identity at the nucleotide level and 100% identity at the amino acid level, annotated as ro02104.

Complementation of the *tadA*::Tn*5* mutant. To demonstrate that the observed phenotype was the result of the mapped transposon insertion and not a random mutation elsewhere in the chromosome, we expressed the *tadA* gene from the P*smyc* promoter contained on the pDPM78 plasmid. As we have observed significant plasmid instability with this family of vectors in the past, cultures were grown for only 48 h prior to analysis. As can be seen in Fig. 1B and C, 48 h is more than adequate to establish significant TAG biosynthesis and accumulation.

Wild-type *R. opacus* PD630 and the *tadA*::Tn*5* mutant containing either the empty vector pDPM70, the WT TadA-expressing plasmid p*tadA*, or the ΔC-terminal TadA-expressing plasmid p*tadA*ΔC were grown in minimal medium supple-

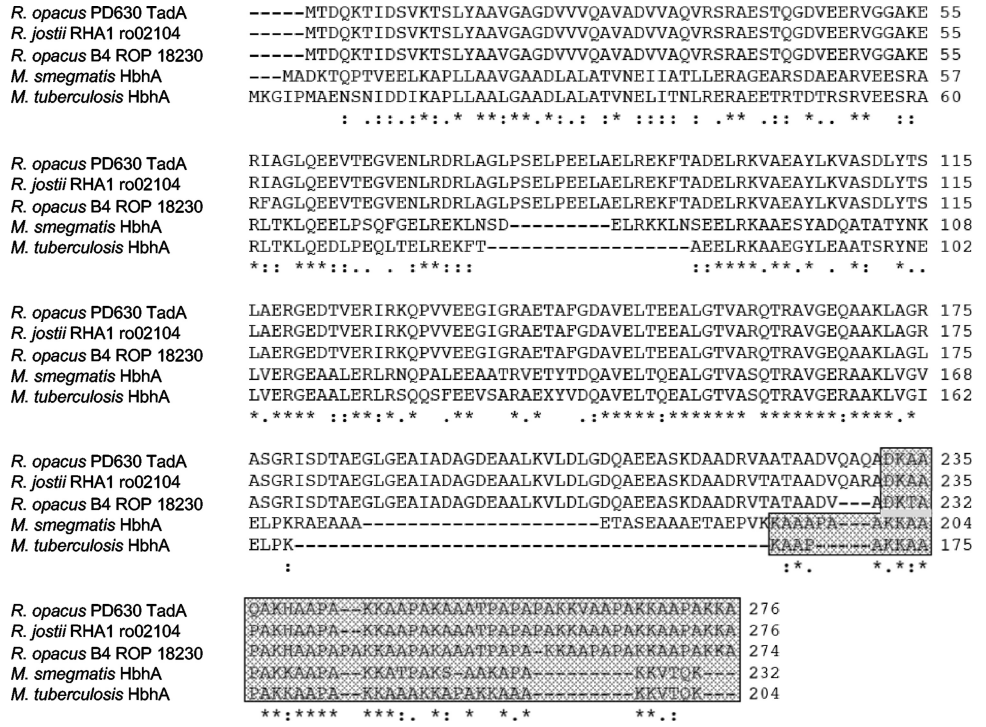

FIG. 2. Alignment of the predicted amino acid sequence of the TadA protein and the mycobacterial heparin-binding hemagglutinin protein (HbhA). The predicted amino acid sequence of the TadA protein from *R. opacus* PD630, the ro02104 protein from *R. jostii* RHA1, the ROP 18230 protein from *Rhodococcus opacus* B4, and the HbhA protein from *M. smegmatis* MC2 155 and *M. tuberculosis* CDC1551 were aligned using ClustalW. The predicted lysine-rich heparin-binding domains are highlighted in gray. The region deleted in the ΔC terminus of TadA mutants is highlighted in gray.

mented with gentamicin for 48 h prior to being diluted 1:10 into baffled flasks containing the same medium. Cultures were then incubated at 30°C with shaking for 48 h prior to harvesting. TAG production was assayed using TLC (Fig. 1C) and GC-FAMES. Additionally, we monitored bacterial growth by assessing CFU counts and observed no difference in the final numbers of bacteria for each culture (data not shown). We observed that extrachromosomal expression of the wild-type *tadA* gene in the 19A3 mutant strain resulted in an increase in TAG accumulation, thus complementing the observed phenotype, while expression of the ΔC-terminus mutant of *tadA* did not have any impact on TAG accumulation (Fig. 1C). To further support these findings, we performed GC-FAMES analysis on cultures grown under identical conditions. Consistent with our TLC analysis, we found that the wild type harboring the empty vector accumulated 31.11% (±0.97%) FAMES/CDW, while the *tadA* mutant containing the empty vector accumulated 21.67% (±0.93%) FAMES/CDW. The *tadA* mutant harboring the vector expressing *tadA* accumulated 29.48% (±1.03%) FAMES/CDW, demonstrating that expression of the *tadA* gene complements the *tadA*::Tn*5* mutant. Additionally, we found that expression of the TadA protein lacking the C terminus was incapable of complementing the *tadA* mutant with this strain, accumulating 22.69% (±1.00%) FAMES/CDW.

Lipid bodies in the *tadA* mutant are morphologically different than those formed in the parental strain. To better assess the TAG accumulation deficiency observed with the *tadA* mutant, we utilized fluorescence microscopy to visualize lipid bodies formed in the wild type and mutant containing the empty vector pDPM70. Cultures of both strains were grown in minimal medium supplemented with gentamicin for 48 h, and lipid bodies were stained with the lipophilic fluorophore Nile Red. We observed that lipid bodies formed in the *tadA* mutant were morphologically different than those formed by the wild type. As shown in Fig. 3, the wild type has numerous small lipid bodies which virtually fill the cytoplasm of the cell, while the *tadA* mutant is characterized by fewer, but slightly larger, lipid bodies. Additionally, the mutant lipid bodies have a sharper appearance, with more delineated edges than those seen with the wild-type bacterium.

With the demonstration that the TAG deficiency observed with the *tadA* mutant was most likely the result of a defect in the lipid body formation pathway, we hypothesized that overexpression of the *tadA* gene in the parental strain, shown above to complement the mutant phenotype, would result in increased lipid body size. To this end, we expressed the wild-type TadA protein as well as the ΔC-terminal TadA in wild-type *R. opacus* and the *tadA*::Tn*5* mutant. Interestingly, overexpression of the *tadA* gene in the wild type resulted in the formation of large lipid bodies, while the truncated TadA had no effect (Fig. 3). As predicted by our TLC analysis, expression of the wild-type TadA protein in the 19A3 mutant resulted in wild-type-like lipid bodies, while the ΔC-terminus variant of TadA did not appear to complement the mutant lipid body phenotype.

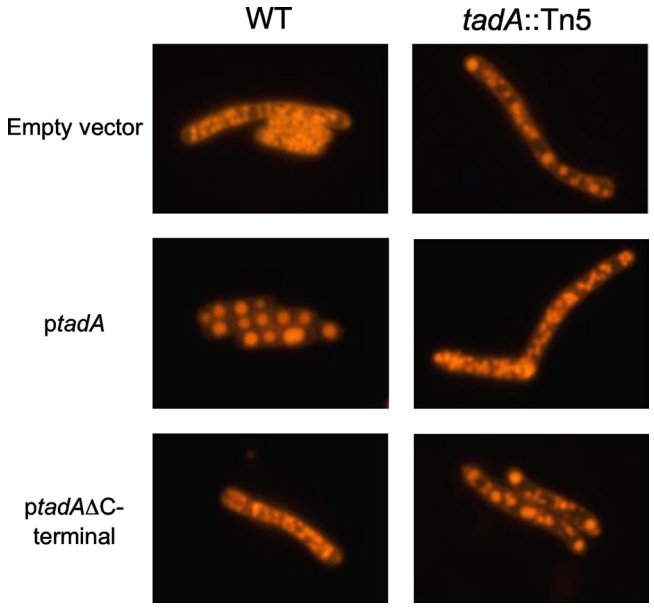

FIG. 3. The *tadA*::Tn*5* mutant demonstrates altered lipid body morphology. Micrographs of bacteria stained with the lipophilic fluorophore Nile Red. Shown are the wild-type *R. opacus* (left) and the *tadA*::Tn*5* mutant (right) strains containing the empty vector pDPM70 or expressing either wild-type *tadA* (p*tadA*) or the C-terminally truncated *tadA* (p*tadA*ΔC) gene were grown in minimal medium for 48 h.

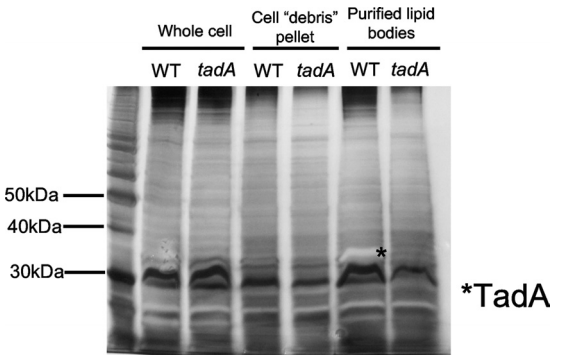

FIG. 4. TadA is enriched in lipid body-containing cellular fractions. Wild-type *R. opacus* and the *tadA*::Tn*5* (*tadA*) mutant were grown in minimal medium for 120 h followed by lysis. Lysates were fractionated using centrifugation. Samples of the unlysed cells, the cellular material depleted of lipid bodies (cell "debris" pellet), and the purified lipid bodies were normalized to the total protein concentration and then resolved using SDS-PAGE followed by silver staining.

TadA localizes to lipid bodies. With the demonstration that expression of the *tadA* gene is linked to lipid body morphology, we hypothesized that it may act to structurally regulate lipid body formation or maturation. Key to this hypothesis would be localization of the TadA protein to lipid bodies. To assess the localization of the TadA protein, specifically to determine whether the protein localizes to lipid bodies, we purified lipid bodies from both the wild type and the *tadA* mutant as previously described (25). Both the wild type and the *tadA*::Tn*5* mutant were grown under TAG-inducing conditions, and lipid bodies were harvested. SDS-PAGE analysis of the lipid body fraction showed a highly enriched protein present in the wild-type strain that was conspicuously absent in the mutant (Fig. 4, asterisk). Mass spectrometric analysis of this band identified it as being the TadA protein, suggesting that the TadA protein localizes to lipid bodies.

TadA binds heparin *in vitro*. As shown in Fig. 2, the TadA protein shares a high level of similarity with the HBHA family of proteins from mycobacteria at the amino acid level. Of particular interest was the high level of similarity at the predicted C-terminal end of the protein, which in *Mycobacterium smegmatis* and other mycobacteria has been shown to be essential for heparin-binding activity both *in vitro* and *in vivo*. Based on these similarities as well as previous data for various mycobacteria, we hypothesized that the TadA protein may also possess heparin-binding activity.

To test whether the TadA protein was capable of binding heparin, we expressed a TadA hexahistidine fusion protein in *E. coli* and purified the protein via nickel-affinity chromatography. Following purification, TadA was incubated with heparin-Sepharose and heparin binding was assessed. As can be seen in Fig. 5, while some of the protein did not bind to the heparin-Sepharose, as indicated by the presence of the TadA protein in the flowthrough fraction, the majority of the protein was found associated with the heparin-Sepharose ("beads").

As previous studies have demonstrated that heparin-binding activity is mediated by the C-terminal, lysine-rich region of heparin-binding hemagglutinins, we proposed that this would also be the case for the TadA protein. To this end, we constructed and purified a variant of the TadA protein which had been truncated at amino acid 231 (ΔC-terminus TadA), thus eliminating the 11 lysine residues found in the C terminus, and assessed its ability to bind to heparin-Sepharose. Abundant levels of the TadA protein were observed in the flowthrough fraction, while no protein associated with the heparin matrix was detected, thus suggesting that the C terminus is necessary for heparin binding (Fig. 5). As an additional control, to ensure that the association of TadA with the heparin-Sepharose resin was not the result of a nonspecific interaction, we performed the heparin-binding assay in the presence of pure heparin and found that this completely abrogated any binding of TadA to the heparin-Sepharose matrix (data not shown).

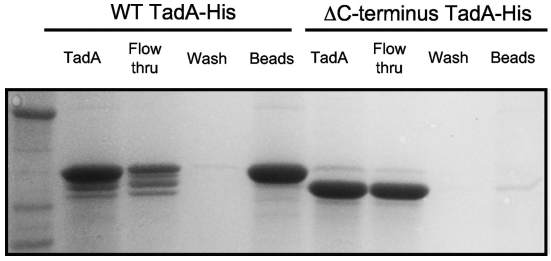

FIG. 5. The TadA protein binds heparin *in vitro*. Wild-type and the ΔC-terminus TadA were purified using nickel affinity chromatography and subsequently assayed for their ability to bind to heparin-Sepharose. Purified TadA was incubated with heparin-Sepharose. Following centrifugation, the supernatant was removed (Flow thru) and the resin was washed 5 times (Wash). The resin was then resuspended in SDS-PAGE loading buffer and boiled (Beads). Samples were resolved using SDS-PAGE and stained with colloidal Coomassie. WT TadA is visible in the heparin-Sepharose fraction, suggesting that it binds to heparin, while the ΔC-terminus mutant was not detected in this fraction.

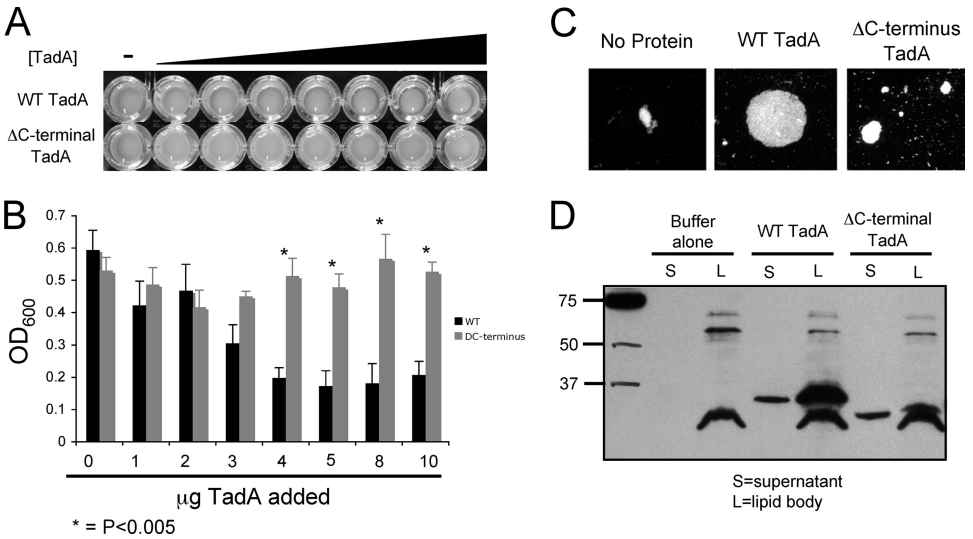

FIG. 6. TadA aggregates purified lipid bodies *in vitro*. (A) TadA agglutinates lipid bodies *in vitro*. Increasing concentrations of purified WT and ΔC-terminus TadA were incubated with purified lipid bodies, resulting in increased sedimentation of the lipid bodies. The concentration of protein in each well corresponds to that shown in the bar graph below. (B) Quantitation of the lipid body aggregation assay. Aliquots were removed from the lipid body aggregation experiments described above, and their absorbance at 600 nm (OD_{600}) was analyzed. Increased concentration of the WT TadA (black bars), and not the ΔC-terminus mutant (gray bars), was associated with a decreased optical density. (C) Fluorescence microscopy of lipid body aggregates from lipid body aggregation assays. Lipid bodies and their aggregates from the lipid body aggregation assay were stained with Nile Red and observed using fluorescence microscopy. Lipid bodies incubated with TadA were found primarily as large aggregates, while lipid bodies incubated with either the buffer control or the ΔC-terminus mutant were primarily observed as medium-sized aggregates. (D) Western blotting of the lipid body aggregation assay. Purified lipid bodies alone (Buffer alone) or lipid bodies incubated with either the wild type or ΔC-terminus TadA protein were pelleted and washed. Supernatant (S) and the lipid body (L) fractions were resolved using SDS-PAGE, transferred, and probed using antihistidine antibodies. Both the wild-type and ΔC-terminal TadA proteins were detected in the lipid body fraction, suggesting that they associate with lipid bodies in this assay.

TadA aggregates purified lipid bodies *in vitro*. Given the demonstration that the absence or overexpression of *tadA* results in altered lipid body formation and the observation that the TadA protein is enriched in lipid body-containing cellular fractions, we sought to demonstrate that the TadA protein could aggregate purified lipid bodies *in vitro*. To this end, we purified lipid bodies from wild-type *R. opacus*, as previously described. Purified lipid bodies were incubated with purified TadA in a round-bottom 96-well dish, in a manner similar to that used for classic hemagglutinin assays. As hypothesized, we observed that wild-type TadA was capable of inducing lipid body aggregation and subsequent flocculation in a dose-dependent manner (Fig. 6A). This activity required the presence of the C-terminal heparin-binding domain, as incubation of purified lipid bodies with the purified ΔC-terminus TadA variant did not result in aggregation. To better quantify this assay, 2 μl of the supernatant from each well was removed, and the optical density at 600 nm was measured. As can be seen in Fig. 6B, the optical density of the supernatants decreases as protein concentration increases, suggesting increased aggregation and flocculation of the lipid bodies with increased concentrations of wild-type TadA. A similar pattern was not observed for the ΔC-terminus mutant, further supporting the hypothesis that the C terminus is essential for lipid body aggregation.

We speculated that this increased flocculation was the result of increased aggregation of the lipid bodies in the presence of TadA. To address this, we observed samples from the various wells using fluorescence microscopy. Lipid bodies from the aggregation experiments were stained with the lipophilic fluorophore Nile Red. We found for both the no-protein control and the lipid bodies incubated with the ΔC-terminal variant of TadA that the lipid bodies existed primarily as small- to medium-sized aggregates. However, when the lipid bodies incubated with wild-type TadA were observed, we found that the lipid bodies had aggregated into very large clumps, often filling the field of view (Fig. 6C).

As we believe that the TadA protein localizes to lipid bodies *in vivo* and that the aggregation activity is dependent on this localization, we wanted to determine if indeed the TadA protein added to the purified lipid bodies during the aggregation assays was associating with the lipid bodies. Conveniently, as the TadA used in these assays contains a hexahistidine tag, we were able to use antipentahistidine antibodies to probe the lipid bodies used in the aggregation assays for the presence of the added, recombinant TadA. Lipid bodies from the aggregation assay were harvested, supernatants were removed, and the lipid bodies were washed prior to resolving both the supernatant and lipid body fractions using SDS-PAGE followed by Western blotting. We observed that both the wild-type TadA and the ΔC-terminus mutant TadA were detected in both the supernatant and the lipid body fractions, suggesting that they associate with lipid bodies during the assay (Fig. 6D).

DISCUSSION

Numerous studies have sought to identify the mechanisms by which various carbon storage molecules are compartmentalized within the cell. Much attention has been given to the PHA storage pathways and the phasins that mediate the for-

mation of the PHA granules. Indeed, it is well documented that PHA storage and granule formation is a regulated and ordered process (44, 45). In oleaginous seeds and plants, oleosins have been implicated in playing a role in lipid body formation (32, 46). However, despite several studies, there is a relative dearth of knowledge concerning the topic for oleaginous bacteria, such as *R. opacus*. This gap in knowledge has led some to speculate that the process of lipid body formation is not regulated but is simply the result of TAG accumulating and blebbing from the cytoplasmic membrane in a disordered and random manner (38). Previous attempts to purify lipid bodies from *R. opacus* and identify proteins associated with them yielded several promising candidates, but little has followed on these initial reports (25). Interestingly, in these earlier reports, the TadA protein was not identified. The discrepancy between our data and those reported in previous works could be the result of different carbon sources provided in the medium (gluconate versus glucose) or other culture conditions, but as we believe TadA plays a structural role and not an enzymatic one in lipid storage, we believe that this is not the case.

Our initial genetic screening identified the 19A3 transposon mutant, which accumulated approximately 35% less TAG than did the wild-type strain. Mapping of the mutation revealed a transposon insertion of ~150 nucleotides into the 5′ end of a gene, which we have since termed *tadA.* Additionally, we identified two other mutants with Tn*5* insertions within the *tadA* gene. All of the mutants isolated demonstrated a similar decrease in TAG accumulation and a similar lipid body phenotype (data not shown). The *tadA* gene is predicted to encode a conserved hypothetical protein with significant sequence similarity to that of the HBHA protein from mycobacteria. This mutation did not appear to have any effect on the growth rate, sugar metabolism, or nitrogen utilization, nor did it seem to have any effect on the metabolism of other lipids, as evidenced by our TLC analysis of this strain (Fig. 1B). We did, however, observe a distinct change in the lipid body morphology for this mutant compared to that of the wild type. Lipid bodies appeared to be slightly larger in the mutant, especially at early time points (Fig. 2). At later time points, we found that lipid bodies in the wild type had begun to coalesce into larger lipid bodies (data not shown), consistent with earlier reports, while in the mutant, the size and shape of the lipid bodies was unchanged. Furthermore, overexpression of the TadA protein in the wild-type strain resulted in the formation of very large lipid bodies (Fig. 2). Thus, it would seem that the TadA protein plays a role in lipid body assembly and/or formation and most likely not in lipid biosynthesis itself. It is interesting that the disruption of the *tadA* gene results in the formation of slightly larger lipid bodies than those seen for the wild type, while overexpression of the TadA protein results in the formation of very large lipid bodies *in vivo*. It is possible that the TadA protein works in concert with other proteins or molecules to mediate lipid body formation; thus, the loss of one component, in this case TadA, may result in altered lipid body formation—slightly larger lipid bodies in this case. As we see that overexpression of the TadA protein leads to much larger lipid bodies, it would be reasonable to conclude that the TadA concentration is a limiting factor in lipid body formation *in vivo*, i.e., the other proteins or molecules necessary for lipid body formation are in relative abundance, and TadA is limiting. Assuming that these other molecules or proteins are not terribly costly for the cell to manufacture, this would be a reasonable mechanism through which the bacterium regulates lipid body formation and maturation. Identification of these additional components may illuminate a complex series of protein-protein interactions that lead to appropriately timed lipid body formation.

Interestingly, the biochemical activity of TadA requires the heparin-binding capability of the protein. Loss of the C-terminal heparin-binding domain results not only in an inability to bind heparin *in vitro* (Fig. 5) but also in an inability to function *in vivo*, as evidenced by the inability of the truncated protein to complement the 19A3 mutant or induce the overexpression phenotype in the wild-type strain (Fig. 1C and 2). Furthermore, despite localizing to purified lipid bodies *in vitro*, the ΔC-terminal TadA protein was incapable of inducing lipid body aggregation in our *in vitro* assay (Fig. 6). We do not believe that the observed lack of activity in the ΔC-terminal mutein is due to improper folding of the protein, as crystallographic studies of the HbhA protein from *Mycobacterium tuberculosis* demonstrated that deletion of the C terminus did not destabilize the protein (16).

It is noteworthy that the TadA homolog HbhA is found in both pathogenic and nonpathogenic mycobacteria and has previously been shown to act as a virulence factor in *Mycobacterium tuberculosis* and *Mycobacterium leprae*, for which it is believed to promote dissemination during early stages of infection (13, 30). Interestingly, *M. tuberculosis* has been shown to accumulate TAG and store it in conspicuous inclusion bodies, similar to those seen for *Rhodococcus* (12, 19, 20). In *M. tuberculosis*, lipid biosynthesis and storage has been linked to pathogenesis (12, 19, 20, 36). It is possible that much like TadA in *Rhodococcus*, HBHA in mycobacteria serves to facilitate lipid body formation and maturation in addition to its predicted role in cytoadherence and dissemination.

While we have demonstrated that the TadA protein does regulate lipid body assembly and/or maturation both *in vivo* and *in vitro* and does so by associating with the lipid bodies, we still are not entirely certain of its exact function *in vivo*. The activity of the C-terminal heparin-binding domain is critical for TadA functionality both *in vivo* and *in vitro*, suggesting that the protein may interact with a lipid body-associated polyanion *in vivo*, thus nucleating lipid bodies and allowing for their previously observed coalescence during later stages of lipid storage. The identity and nature of this structure remain elusive and warrant future investigation.

Thus, we have presented here the first demonstration of a protein that not only localizes to lipid bodies in bacteria but also acts to mediate their assembly and/or maturation. Based on these data, we predict that the process of lipid body assembly and maturation, much like numerous other cellular processes, is highly regulated. Most likely, numerous proteins acting in unison mediate this process.

ACKNOWLEDGMENTS

We thank Christopher J. Brigham, Robert M. Q. Shanks, and Daniel E. Kadouri for critical reviews of the manuscript. We thank the Dianne K. Newman laboratory for the use of its microscope.

This work has been supported by grants from Shell International Exploration & Production, Inc., and a seed grant from the Massachusetts Institute of Technology Energy Initiative (MITei).

REFERENCES

1. **Alvarez, A. F., H. M. Alvarez, R. Kalscheuer, M. Waltermann, and A. Steinbuchel.** 2008. Cloning and characterization of a gene involved in triacylglycerol biosynthesis and identification of additional homologous genes in the oleaginous bacterium *Rhodococcus opacus* PD630. Microbiology **154:**2327–2335.
2. **Alvarez, H. M., R. Kalscheuer, and A. Steinbuchel.** 2000. Accumulation and mobilization of storage lipids by *Rhodococcus opacus* PD630 and *Rhodococcus ruber* NCIMB 40126. Appl. Microbiol. Biotechnol. **54:**218–223.
3. **Alvarez, H. M., F. Mayer, D. Fabritius, and A. Steinbuchel.** 1996. Formation of intracytoplasmic lipid inclusions by *Rhodococcus opacus* strain PD630. Arch. Microbiol. **165:**377–386.
4. **Alvarez, H. M., M. F. Souto, A. Viale, and O. H. Pucci.** 2001. Biosynthesis of fatty acids and triacylglycerols by 2,6,10,14-tetramethyl pentadecane-grown cells of *Nocardia globerula* 432. FEMS Microbiol. Lett. **200:**195–200.
5. **Alvarez, H. M., and A. Steinbuchel.** 2002. Triacylglycerols in prokaryotic microorganisms. Appl. Microbiol. Biotechnol. **60:**367–376.
6. **Arabolaza, A., E. Rodriguez, S. Altabe, H. Alvarez, and H. Gramajo.** 2008. Multiple pathways for triacylglycerol biosynthesis in *Streptomyces coelicolor*. Appl. Environ. Microbiol. **74:**2573–2582.
7. **Bertani, G.** 2004. Lysogeny at mid-twentieth century: P1, P2, and other experimental systems. J. Bacteriol. **186:**595–600.
8. **Bligh, E. G., and W. J. Dyer.** 1959. A rapid method of total lipid extraction and purification. Can. J. Biochem. Physiol. **37:**911–917.
9. **Brandl, H., R. A. Gross, R. W. Lenz, and R. C. Fuller.** 1988. *Pseudomonas oleovorans* as a source of poly(beta-hydroxyalkanoates) for potential applications as biodegradable polyesters. Appl. Environ. Microbiol. **54:**1977–1982.
10. **Burnette, W. N.** 1981. "Western blotting": electrophoretic transfer of proteins from sodium dodecyl sulfate-polyacrylamide gels to unmodified nitrocellulose and radiographic detection with antibody and radioiodinated protein A. Anal. Biochem. **112:**195–203.
11. **Daniel, J., C. Deb, V. S. Dubey, T. D. Sirakova, B. Abomoelak, H. R. Morbidoni, and P. E. Kolattukudy.** 2004. Induction of a novel class of diacylglycerol acyltransferases and triacylglycerol accumulation in *Mycobacterium tuberculosis* as it goes into a dormancy-like state in culture. J. Bacteriol. **186:**5017–5030.
12. **Deb, C., C. M. Lee, V. S. Dubey, J. Daniel, B. Abomoelak, T. D. Sirakova, S. Pawar, L. Rogers, and P. E. Kolattukudy.** 2009. A novel in vitro multiple-stress dormancy model for *Mycobacterium tuberculosis* generates a lipid-loaded, drug-tolerant, dormant pathogen. PLoS One **4:**e6077.
13. **de Lima, C. S., M. A. Marques, A. S. Debrie, E. C. Almeida, C. A. Silva, P. J. Brennan, E. N. Sarno, F. D. Menozzi, and M. C. Pessolani.** 2009. Heparin-binding hemagglutinin (HBHA) of *Mycobacterium leprae* is expressed during infection and enhances bacterial adherence to epithelial cells. FEMS Microbiol. Lett. **292:**162–169.
14. **Downing, D. T.** 1968. Photodensitometry in the thin-layer chromatographic analysis of neutral lipids. J. Chromatogr. **38:**91–99.
15. **Ehrt, S., X. V. Guo, C. M. Hickey, M. Ryou, M. Monteleone, L. W. Riley, and D. Schnappinger.** 2005. Controlling gene expression in mycobacteria with anhydrotetracycline and Tet repressor. Nucleic Acids Res. **33:**e21.
16. **Esposito, C., M. V. Pethoukov, D. I. Svergun, A. Ruggiero, C. Pedone, E. Pedone, and R. Berisio.** 2008. Evidence for an elongated dimeric structure of heparin-binding hemagglutinin from *Mycobacterium tuberculosis*. J. Bacteriol. **190:**4749–4753.
17. **Fishbein, W. N.** 1972. Quantitative densitometry of 1–50 g protein in acrylamide gel slabs with Coomassie blue. Anal. Biochem. **46:**388–401.
18. **Fowler, S. D., and P. Greenspan.** 1985. Application of Nile red, a fluorescent hydrophobic probe, for the detection of neutral lipid deposits in tissue sections: comparison with oil red O. J. Histochem Cytochem. **33:**833–836.
19. **Garton, N. J., H. Christensen, D. E. Minnikin, R. A. Adegbola, and M. R. Barer.** 2002. Intracellular lipophilic inclusions of mycobacteria *in vitro* and in sputum. Microbiology **148:**2951–2958.
20. **Garton, N. J., S. J. Waddell, A. L. Sherratt, S. M. Lee, R. J. Smith, C. Senner, J. Hinds, K. Rajakumar, R. A. Adegbola, G. S. Besra, P. D. Butcher, and M. R. Barer.** 2008. Cytological and transcript analyses reveal fat and lazy persister-like bacilli in tuberculous sputum. PLoS Med. **5:**e75.
21. **Greenspan, P., E. P. Mayer, and S. D. Fowler.** 1985. Nile red: a selective fluorescent stain for intracellular lipid droplets. J. Cell Biol. **100:**965–973.
22. **Han, J., Q. Lu, L. Zhou, H. Liu, and H. Xiang.** 2009. Identification of the polyhydroxyalkanoate (PHA)-specific acetoacetyl coenzyme A reductase among multiple FabG paralogs in *Haloarcula hispanica* and reconstruction of the PHA biosynthetic pathway in *Haloferax volcanii*. Appl. Environ. Microbiol. **75:**6168–6175.
23. **Hoffman, C. S., and F. Winston.** 1987. A ten-minute DNA preparation from yeast efficiently releases autonomous plasmids for transformation of *Escherichia coli*. Gene **57:**267–272.
24. **Jendrossek, D.** 2009. Polyhydroxyalkanoate granules are complex subcellular organelles (carbonosomes). J. Bacteriol. **191:**3195–3202.
25. **Kalscheuer, R., M. Waltermann, M. Alvarez, and A. Steinbuchel.** 2001. Preparative isolation of lipid inclusions from *Rhodococcus opacus* and *Rhodococcus ruber* and identification of granule-associated proteins. Arch. Microbiol. **177:**20–28.
26. **King, R. J., H. Martin, D. Mitts, and F. M. Holmstrom.** 1977. Metabolism of the apoproteins in pulmonary surfactant. J. Appl. Physiol. **42:**483–491.
27. **Kurosawa, K., P. Boccazzi, N. de Almeida, and A. J. Sinskey.** 2010. High-cell-density batch fermentation of *Rhodococcus opacus* PD630 using a high glucose concentration for triacylglycerol production. J. Biotechnol. **147:**212–218.
28. **Laemmli, U. K.** 1970. Cleavage of structural proteins during the assembly of the head of bacteriophage T4. Nature **227:**680–685.
29. **MacEachran, D. P., S. Ye, J. M. Bomberger, D. A. Hogan, A. Swiatecka-Urban, B. A. Stanton, and G. A. O'Toole.** 2007. The *Pseudomonas aeruginosa* secreted protein PA2934 decreases apical membrane expression of the cystic fibrosis transmembrane conductance regulator. Infect. Immun. **75:**3902–3912.
30. **Pethe, K., S. Alonso, F. Biet, G. Delogu, M. J. Brennan, C. Locht, and F. D. Menozzi.** 2001. The heparin-binding haemagglutinin of M. tuberculosis is required for extrapulmonary dissemination. Nature **412:**190–194.
31. **Petty, K. J.** 2001. Metal-chelate affinity chromatography, Unit 9.4. *In* J. E. Coligan et al. (ed.), Current protocols in protein science. John Wiley & Sons, New York, NY.
32. **Purkrtova, Z., P. Jolivet, M. Miquel, and T. Chardot.** 2008. Structure and function of seed lipid-body-associated proteins. C. R. Biol. **331:**746–754.
33. **Rehm, B. H., and A. Steinbuchel.** 1999. Biochemical and genetic analysis of PHA synthases and other proteins required for PHA synthesis. Int. J. Biol. Macromol. **25:**3–19.
34. **Shanks, R. M., N. C. Caiazza, S. M. Hinsa, C. M. Toutain, and G. A. O'Toole.** 2006. *Saccharomyces cerevisiae*-based molecular tool kit for manipulation of genes from gram-negative bacteria. Appl. Environ. Microbiol. **72:**5027–5036.
35. **Shanks, R. M., D. E. Kadouri, D. P. MacEachran, and G. A. O'Toole.** 2009. New yeast recombineering tools for bacteria. Plasmid **62:**88–97.
36. **Sirakova, T. D., V. S. Dubey, C. Deb, J. Daniel, T. A. Korotkova, B. Abomoelak, and P. E. Kolattukudy.** 2006. Identification of a diacylglycerol acyltransferase gene involved in accumulation of triacylglycerol in *Mycobacterium tuberculosis* under stress. Microbiology **152:**2717–2725.
37. **Stephanou, N. C., F. Gao, P. Bongiorno, S. Ehrt, D. Schnappinger, S. Shuman, and M. S. Glickman.** 2007. Mycobacterial nonhomologous end joining mediates mutagenic repair of chromosomal double-strand DNA breaks. J. Bacteriol. **189:**5237–5246.
38. **Waltermann, M., A. Hinz, H. Robenek, D. Troyer, R. Reichelt, U. Malkus, H. J. Galla, R. Kalscheuer, T. Stoveken, P. von Landenberg, and A. Steinbuchel.** 2005. Mechanism of lipid-body formation in prokaryotes: how bacteria fatten up. Mol. Microbiol. **55:**750–763.
39. **Waltermann, M., H. Luftmann, D. Baumeister, R. Kalscheuer, and A. Steinbuchel.** 2000. *Rhodococcus opacus* strain PD630 as a new source of high-value single-cell oil? Isolation and characterization of triacylglycerols and other storage lipids. Microbiology **146:**1143–1149.
40. **Waltermann, M., and A. Steinbuchel.** 2005. Neutral lipid bodies in prokaryotes: recent insights into structure, formation, and relationship to eukaryotic lipid depots. J. Bacteriol. **187:**3607–3619.
41. **Waltermann, M., T. Stoveken, and A. Steinbuchel.** 2007. Key enzymes for biosynthesis of neutral lipid storage compounds in prokaryotes: properties, function and occurrence of wax ester synthases/acyl-CoA: diacylglycerol acyltransferases. Biochimie **89:**230–242.
42. **Walde, E.** 1962. Untersuchungen uber Wachstum und Speicherstoffsynthese von Hydrogenomonas. Arch. Mikrobiol. **43:**109–137.
43. **Yang, J. C., P. A. Lessard, and A. J. Sinskey.** 2007. Characterization of the mobilization determinants of pAN12, a small replicon from *Rhodococcus erythropolis* AN12. Plasmid **57:**71–81.
44. **York, G. M., B. H. Junker, J. A. Stubbe, and A. J. Sinskey.** 2001. Accumulation of the PhaP phasin of *Ralstonia eutropha* is dependent on production of polyhydroxybutyrate in cells. J. Bacteriol. **183:**4217–4226.
45. **York, G. M., J. Stubbe, and A. J. Sinskey.** 2001. New insight into the role of the PhaP phasin of *Ralstonia eutropha* in promoting synthesis of polyhydroxybutyrate. J. Bacteriol. **183:**2394–2397.
46. **Zweytick, D., K. Athenstaedt, and G. Daum.** 2000. Intracellular lipid particles of eukaryotic cells. Biochim. Biophys. Acta **1469:**101–120.